Molecular Pharmacology Fast Forward. Published on September 29, 2014 as DOI: 10.1124/mol.114.094698
This article has not been copyedited and formatted. The final version may differ from this version.

Studies on an acetylcholine binding protein identify a basic residue in loop G on the β1-strand as a new structural determinant of neonicotinoid actions

Makoto Ihara, Toshihide Okajima, Atsuko Yamashita, Takuma Oda, Takuya Asano, Mikana Matsui, David B. Sattelle and Kazuhiko Matsuda

Department of Applied Biological Chemistry, Faculty of Agriculture, Kinki University, 3327-204 Naka-machi, Nara 631-8505, Japan (M.I., T.O., T.A., M.M., K.M.)

Institute of Scientific and Industrial Research, Osaka University, 8-1 Mihogaoka, Ibaraki, Osaka 567-0047, Japan (T.O.)

Graduate School of Medicine, Dentistry and Pharmaceutical Sciences, Okayama University, 1-1-1 Tsushima-naka, Kita-ku, Okayama 700-8530, Japan (A.Y.)

The Wolfson Institute for Biomedical Research, Department of Medicine, Cruciform Building, University College London, Gower Street, London, WC1E 6BT, United Kingdom (D.B.S.)

Primary laboratory origin: Department of Applied Biological Chemistry, Faculty of Agriculture, Kinki University

Molecular Pharmacology Fast Forward. Published on September 29, 2014 as DOI: 10.1124/mol.114.094698
This article has not been copyedited and formatted. The final version may differ from this version.

Running title: Structural determinants of neonicotinoid actions

To whom correspondence should be addressed: Makoto Ihara or Kazuhiko Matsuda
Department of Applied Biological Chemistry, Faculty of Agriculture, Kinki University
3327-204 Nakamachi, Nara 631-8505, Japan
Makoto Ihara Tel: +81-742-437010; email: makoto_i@nara.kindai.ac.jp
Kazuhiko Matsuda Tel: +81-742-437153; email: kmatsuda@nara.kindai.ac.jp

Number of text pages	31
Number of tables	3
Number of figures	7
Number of references	49
Number of words in Abstract	222 words
Number of words in Introduction	621 words
Number of words in Discussion	1222 words

Abbreviations: ACh, acetylcholine; nAChR, nicotinic acetylcholine receptor; *Ls*-AChBP, *Lymnaea stagnalis*-acetylcholine binding protein; IMI, imidacloprid; CTD, clothianidin, THI, thiacloprid; CH-IMI, nitromethylene imidacloprid analogue, DN-IMI, desnitro-imidacloprid; HEPES, 4-(2-hydroxyethyl)-1-piperazineethanesulfonic acid; SOS, standard oocyte saline; EC_{50}, half maximal effective concentration; I_{max}, normalized maximal response

Molecular Pharmacology Fast Forward. Published on September 29, 2014 as DOI: 10.1124/mol.114.094698
This article has not been copyedited and formatted. The final version may differ from this version.

Abstract

Neonicotinoid insecticides target insect nicotinic acetylcholine receptors (nAChRs). Their widespread use and possible risks to pollinators make it extremely urgent to understand the mechanisms underlying their actions on insect nAChRs. We therefore elucidated X-ray crystal structures of the *Lymnaea stagnalis* acetylcholine binding protein (*Ls*-AChBP) and its Gln55Arg mutant, more closely resembling insect nAChRs, in complex with a nitromethylene imidacloprid analogue (CH-IMI) and desnitro imidacloprid metabolite (DN-IMI) as well as commercial neonicotinoids, imidacloprid, clothianidin and thiacloprid. Unlike imidacloprid, clothianidin and CH-IMI, thiacloprid did not stack with Tyr185 in the wild-type *Ls*-AChBP, but did in the Gln55Arg mutant, interacting electrostatically with Arg55. In contrast, DN-IMI lacking the NO_2 group was directed away from Lys34 and Arg55 to form hydrogen bonds with Tyr89 in loop A and the main chain carbonyl of Trp143 in loop B. Unexpectedly, we found that several neonicotinoids interacted with Lys34 in loop G on the β1 strand in the crystal structure of the Gln55Arg mutant. Basic residues introduced into the α7 nAChR at positions equivalent to AChBP Lys34 and Arg55 enhanced agonist actions of neonicotinoids, while reducing the actions of acetylcholine, (-)-nicotine and DN-IMI. Thus, not only the basic residues in loop D, but also those in loop G determine the actions of neonicotinoids. These novel findings provide new insights into the modes of action of neonicotinoids and emerging derivatives.

Molecular Pharmacology Fast Forward. Published on September 29, 2014 as DOI: 10.1124/mol.114.094698
This article has not been copyedited and formatted. The final version may differ from this version.

Introduction

Nicotinic acetylcholine receptors (nAChRs) are members of the Cys-loop superfamily of ligand-gated ion-channels (LGICs), and neuronal nAChRs play a central role in fast cholinergic neurotransmission in both vertebrates and invertebrates (Changeux, 2012; Hurst et al., 2013). nAChRs are composed of five subunit protein, and form pentagonal assembly. Subunit proteins consist of an extracellular ligand-binding domain (LBD) and four transmembrane regions (TMs), the second of which (TM2) lines an integral ion channel. Agonists binding sites are formed at the subunit interfaces of the LBD, where historically regions involved in agonist binding are named loops A, B, C, D, E and F (Corringer et al., 2000). The binding of acetylcholine (ACh) to nAChRs triggers gating of the integral cation channel to mediate cholinergic neurotransmissions (Unwin and Fujiyoshi, 2012).

Imidacloprid and several insecticidal imidacloprid analogues (Fig. 1A) have been developed since 1990s and these neonicotinoids made up 20.8% of global insecticide sales of US$15.045 billion/annum in 2012 (PhillipsMcDougall, 2013). Normally neonicotinoids act as nAChR agonists (Casida and Durkin, 2013; Ihara et al., 2003; Ihara et al., 2004; Matsuda et al., 2001; Matsuda et al., 2009; Matsuda et al., 2005; Tomizawa and Casida, 2003; Tomizawa and Casida, 2005), however imidacloprid can also act as an antagonist depending on targeted nAChR subtypes (Ihara et al., 2006; Ihara et al., 2003; Salgado and Saar, 2004). Site-directed mutagenesis, electrophysiology and molecular modeling have pointed to basic residues in loop D together with non-acidic residues in loop C as potential determinants of the selectivity of neonicotinoids for insect over vertebrate nAChRs (Matsuda et al., 2009; Shimomura et al., 2002; Shimomura et al., 2006; Toshima et al., 2009) (Fig. 1B). However, neonicotinoids show no particular selectivity among insect species. Indeed, they may even play a role in “colony collapse disorder (CCD)” of honey bees (Gill et al., 2012; Maus et al., 2003). Also a possible

Molecular Pharmacology Fast Forward. Published on September 29, 2014 as DOI: 10.1124/mol.114.094698
This article has not been copyedited and formatted. The final version may differ from this version.

contribution of neonicotinoids to the declines of insectivorous birds has been reported (Hallmann et al., 2014). Thus, understanding the molecular mechanism of neonicotinoid actions is of considerable importance.

Since AChBP has been widely recognized as a surrogate for the LBD of nAChRs (Rucktooa et al., 2009), we previously elucidated the X-ray crystal structures of the *Lymnaea stagnalis* acetylcholine binding protein (*Ls*-AChBP) (Brejc et al., 2001) in complex with imidacloprid and clothianidin (Ihara et al., 2008). Crystal structures of *Aplysia californica* AChBP (*Ac*-AChBP) in complex with imidacloprid and thiacloprid were also reported (Talley et al., 2008). Both studies agree in two important respects. First, the guanidine moiety of imidacloprid stacks with the tyrosine residue (Tyr185 in *Ls*-AChBP and the equivalent residue Tyr188 in *Ac*-AChBP) in loop C. Secondly, the NO_2 group of imidacloprid forms a hydrogen bond with the glutamine residue (Gln55 for *Ls*-AChBP and Gln57 for *Ac*-AChBP), which is equivalent to the basic residues frequently observed in loop D of insect nAChRs (Fig. 1B, C; see Supplementary Fig. 1 for entire amino acid sequences), accounting, at least in part, for the role of loop D in selective insecticidal actions of neonicotinoids. However, structural and functional studies of more neonicotinoid family members are needed to help build an improved picture of key target-site determinants.

We therefore generated a Gln55Arg *Ls*-AChBP mutant that mimics more closely loop D of the insect nAChR LBD (Fig. 1C), and elucidated the crystal structures of both wild-type and Gln55Arg mutant of *Ls*-AChBPs complexed with desnitro-imidacloprid (DN-IMI) lacking the NO_2 group as well as with several neonicotinoids (Fig. 1A). We also investigated the actions of these same compounds on the homo pentameric avian α7 nAChR (Couturier et al., 1990). This study enhances our understanding of neonicotinoid–target interactions and highlights a role for basic residues in loop G on the β1 strand as well as in loop D on the β2 strand.

Molecular Pharmacology Fast Forward. Published on September 29, 2014 as DOI: 10.1124/mol.114.094698
This article has not been copyedited and formatted. The final version may differ from this version.

Materials and Methods

Chemicals

Imidacloprid, thiacloprid and nitromethylene imidacloprid analogue (CH-IMI) were donated by Bayer CropScience, whereas clothianidin was a gift of Sumitomo Chemical. DN-IMI was synthesized *de novo* as described (Latli et al., 1996). ACh and (-)-nicotine were purchased from Sigma-Aldrich (St. Louis, MO, USA) and used without further purification. Bromine-substituted clothianidin analogue (Br-Clothianidin) was prepared as reported previously (Ihara et al., 2008).

Expression constructs

A *Pichia pastoris* expression system (Life Technologies, Carlsbad, CA, USA) was used for the preparation of the recombinant *Ls*-AChBPs as described previously (Ihara *et al.*, 2008). The *Ls*-AChBP gene was cloned in the pPICZα B vector (Life Technologies, Carlsbad, CA, USA). In this process, the leucine at position 1 was mutated to alanine to adapt the sequence to the Pst I restriction site. The cDNA encoding the chicken α7 nAChR, kindly donated by Prof. Mark Ballivet of Geneva University, was cloned into pcDNA3.1 (+) vector (Ihara et al., 2008). Any mutations to expression constructs were introduced using a QuikChange kit (Agilent Technologies, CA, USA), and all DNA sequences were confirmed using a 3100 Genetic analyzer (Life Technologies).

Protein preparation

Both wild-type and the Gln55Arg mutant of *Ls*-AChBP were expressed in *P. pastoris* X-33 and purified as described previously (Ihara et al., 2008). In brief, proteins secreted by *P. pastoris* X-33 were purified using a Q-Sepharose column (GE Healthcare, Piscataway, NJ, USA) and

Molecular Pharmacology Fast Forward. Published on September 29, 2014 as DOI: 10.1124/mol.114.094698
This article has not been copyedited and formatted. The final version may differ from this version.

subsequently deglycosylated with peptide-*N*-glycosidase F (Wako Pure Chemical Industries, Osaka, Japan) at a concentration of 50 U/mg protein at 37˚C for 24 h. The protein samples were further purified using Mono Q and Superdex 200 columns (GE Healthcare). Purified *Ls*-AChBPs were confirmed by mass spectrometry and N-terminal analysis.

Evaluation of binding of neonicotinoids by Isothermal Titration Calorimetry

Isothermal Titration Calorimetry (ITC) was recorded by an iTC_{200} (GE Healthcare) using 10 μM *Ls*-AChBP and 125 or 250 μM ligands in 25 mM sodium phosphate buffer (pH 8.0) containing 100 mM NaCl at 25ºC. The titration curve was fitted using the manufacturer's software.

Crystallization and X-ray data collection

Purified *Ls*-AChBPs (6.0 mg/mL) were incubated with 0.5 mM neonicotinoids at 4°C for 1 h prior to crystallization. Crystals of *Ls*-AChBP–neonicotinoid complexes were obtained by the vapor diffusion method at 20°C with 1:1 ratio of protein to reservoir solution containing 0.2 M Na citrate pH 5.7, 15-22% PEG3350, and about 0.5 mM of either imidacloprid, clothianidin, Br-clothianidin, thiacloprid, or CH-IMI; 1.5 M Na acetate, 0.05 M $CdSO_4$, 0.1 M HEPES-Na, pH 7.5, and about 0.5 mM of DN-IMI for wild-type complex; 24-27% PEG4000, 0.1-0.3 M Li_2SO_4, 0.1 M Tris-HCl, pH 8.5, and about 0.5 mM DN-IMI for the Gln55Arg mutant complex. The crystals were flash-cooled in liquid nitrogen after soaking in the cryo-protectant solutions containing the reservoir solution comprising 10% higher concentration of the precipitant, supplemented with 20% glycerol and 0.5 mM of each neonicotinoid. X-ray diffraction data sets were collected at 90 or 100 K using either Bruker AXS DIP6040 detector at BL44XU (Yoshimura et al., 2007), ADSC QUANTUM 210 detector at BL44B2 (Adachi et al., 2001), Jupitor210 at BL26B1, or Mar225 at BL26B2 (Ueno et al., 2006) beamlines in SPring-8, and

processed with Mosflm (Leslie, 1992) or HKL2000 (Otwinowski and Minor, 1997). In addition, anomalous data from Br-clothianidin bound to the Gln55Arg mutant *Ls*-AChBP were collected at a wavelength of 0.919 Å to identify the position of the chlorine atom in clothianidin, while those from thiacloprid bound to the wild-type and Gln55Arg mutant *Ls*-AChBP were collected at a wavelength of 1.75 Å to identify the position of the sulfur atom in thiacloprid.

Phase determination and refinement

The structure of wild-type *Ls*-AChBP complexed with DN-IMI was solved by molecular replacement with PHASER (McCoy, 2007) using the coordinate of *Ls*-AChBP–imidacloprid complex (PDB entry: 2ZJU) whose ligands and waters were removed. For the Gln55Arg mutant complexed with DN-IMI, the structure was solved by molecular replacement using MOLREP (Vagin and Teplyakov, 1997) with the coordinate 2ZJU whose waters but not the ligand were removed. For the other neonicotinoids, crystal parameters were quite similar to those of the *Ls*-AChBP–imidacloprid complex (2ZJU), thus initial models were obtained by rigid body refinement with CNS version 1.2 (Brünger et al., 1998) using the coordinates of 2ZJU whose ligands and waters were removed. Subsequently, the initial models were refined with either CNS version 1.2, CCP4 Program version 6.4 (Winn et al., 2011) or PHENIX version 1.9-1691 (Adams et al., 2010). Manual model building was performed on the basis of $2F_o$-F_c, F_o-F_c, and omit maps with Coot (Emsley and Cowtan, 2004). The neonicotinoids and the mutated residue were introduced to the model after the initial refinement. The geometries of all the ligands were validated using Mogul (Bruno et al., 2004). The NCS restraints were initially applied for the refinements and removed at later steps. The details of data collection and refinement statistics are provided in Table 1. Simulated annealing omit maps of bound ligands were calculated using PHENIX. The binding orientations of thiacloprid in the crystals were verified by the sulfur atom

Molecular Pharmacology Fast Forward. Published on September 29, 2014 as DOI: 10.1124/mol.114.094698
This article has not been copyedited and formatted. The final version may differ from this version.

position in the anomalous map, while those of clothianidin were deduced from the bromine atom position in the anomalous map for the bound Br-clothianidin. Figures are generated by PyMOL (Schrödinger, New York, NY, USA) and each interface of five interfaces in crystals was named according to the chain names in the coordinates.

Functional expression of α7 nAChR and electrophysiology

Xenopus laevis oocytes at stage V or VI were used for expression of the avian α7 nAChR (Couturier et al., 1990). Functional expression was achieved by injecting cDNA encoding nAChR gene as previously described (Ihara et al., 2003; Shimomura et al., 2002). Robust currents were obtained without the need to co-express the RIC-3 (Miller et al., 1996; Nguyen et al., 1995) with α7 nAChR. *Xenopus* oocytes were perfused extracellularly with a standard oocyte saline containing 100 mM NaCl, 2 mM KCl, 1.8 mM $CaCl_2$, 1 mM $MgCl_2$ and 5 mM HEPES 5.0 (pH 7.6). Atropine (0.5 μM) was added to SOS to suppress any muscarinic response of oocytes. Membrane currents evoked by agonist application were recorded using a GeneClamp 500B amplifier and Digidata 1200 digitizer with pClamp 8 software (Molecular Devices, Sunnyvale, CA, USA). The peak current amplitude of the response of wild-type and mutant α7 to ligands tested was normalized to that of the ACh-induced response at concentrations where concentration-response curves reached a maximum. Data was processed using pClamp 9 software (Molecular Devices) and analyzed by non-linear regression analysis using Prism 4 (GraphPad Software, La Jolla, CA, USA) to obtain half maximal concentration EC_{50} (M) and normalized maximal response I_{max} (Ihara et al., 2003; Shimomura et al., 2002).

Molecular Pharmacology Fast Forward. Published on September 29, 2014 as DOI: 10.1124/mol.114.094698
This article has not been copyedited and formatted. The final version may differ from this version.

Results

Structures of AChBP complexed with neonicotinoids and analogues

We co-crystallized the wild-type and Gln55Arg mutant *Ls*-AChBPs with commercial neonicotinoids (imidacloprid, clothianidin and thiacloprid) and a nitromethylene imidacloprid analogue CH-IMI (Fig. 1A) excluding only the wild-type *Ls*-AChBPs in complex with imidacloprid and clothianidin which were reported earlier (Ihara et al., 2008). These crystals in complex with commercial neonicotinoids and CH-IMI belong to the same space group, $P6_5$. We also co-crystallized wild-type and Gln55Arg mutant *Ls*-AChBPs with the denitrated imidacloprid metabolite DN-IMI, and obtained crystals belonging to space group $P2_12_12_1$. The crystal structures were solved and refined at 2.09–2.68Å resolution (Table 1). Common to other AChBP structures reported, a pentameric ring structure with a center aperture was obtained for all complexes (Fig. 1D). Electron density of ligand-omit maps (Fig. 2) indicated that all five LBDs were occupied by a single ligand, and no empty binding site was observed. The model for clothianidin interacting with the binding site was confirmed with anomalous peaks observed at the bromine atom from Br-clothianidin complexed with the Gln55Arg mutant of the *Ls*-AChBP in the X-ray diffraction data collected at 0.919 Å (Fig. 2B and Table 1), as in the wild-type protein (Ihara et al., 2008), allowing unequivocal determination of the ring orientation, because the ring structure of clothianidin with its substituent groups is asymmetric. In the case for thiacloprid modeling, anomalous peaks observed in the X-ray diffraction data, which were collected at 1.75 Å for the wild-type and mutant *Ls*-AChBP complexes (Table 1), indicated the sulfur and chlorine atom positions in thiacloprid along with the sulfur atom position in Met114 (Fig. 2C), and thus permit unambiguous determination of the thiacloprid binding mode. The stereochemical geometries for all the bound ligands were verified by Mogul (Bruno et al., 2004) (Table 1 and Supplementary Tables 1–10).

Molecular Pharmacology Fast Forward. Published on September 29, 2014 as DOI: 10.1124/mol.114.094698
This article has not been copyedited and formatted. The final version may differ from this version.

There were no large structural differences observed at the aromatic ring system of the neonicotinoids and the surrounding amino acid residues in the *Ls*-AChBP between the wild-type and Gln55Arg, as well as among all the tested neonicotinoids (Figs. 2, 3 and Supplementary Fig. 2). The aromatic ring moiety of thiacloprid formed a hydrogen bond at the nitrogen atom via a single water molecule associated with the main chain amide (both NH and C=O) of Met114 and the main chain carbonyl of Leu102 in loop E (Supplementary Fig. 2A), as also seen in imidacloprid, clothianidin (Ihara et al., 2008; Talley et al., 2008), CH-IMI (Supplementary Fig. 2B) and DN-IMI (Supplementary Fig. 2C).

Interactions of the guanidine and related moieties with wild-type AChBP

We previously reported that the guanidine moiety of imidacloprid and clothianidin stacked with Tyr185 in loop C, while the hydrogen atoms of the ethylene bridge of imidacloprid and the *N*-methyl group of clothianidin underwent CH-π interactions (Nishio, 2006) with the aromatic ring of Trp143 in loop B in the wild-type *Ls*-AChBP (Fig. 3A, D) (Ihara et al., 2008). In addition, we showed that the NO_2 group of imidacloprid (Fig. 3A), but not of clothianidin (Fig. 3D), formed a hydrogen bond with Gln55 (Ihara et al., 2008). Here we provide evidence that thiacloprid does not stack with Tyr185 in the wild-type protein, but instead interacts with Tyr89 in loop A, Trp143 in loop B, Tyr192 in loop C and Trp53 in loop D, while forming a hydrogen bond between the CN group and the main chain amide of Tyr185 (Fig. 3G). In a similar way to imidacloprid, the nitromethylene imidacloprid analogue CH-IMI stacked with Tyr185, while forming a hydrogen bond at the NO_2 group with Gln55 (Fig. 3J). In addition, CH-IMI interacted with Lys34 on the β1 strand (not shown in Fig. 3J. See below for details).

We also investigated the binding characteristics of neonicotinoids by isothermal titration calorimetry (ITC, see Supplementary Fig. 3 for titration curves). CH-IMI showed the highest

Molecular Pharmacology Fast Forward. Published on September 29, 2014 as DOI: 10.1124/mol.114.094698
This article has not been copyedited and formatted. The final version may differ from this version.

affinity (K_d = 92 nM) of all the neonicotinoids tested. Thiacloprid bound to the wild-type protein more strongly (K_d = 297 nM) than imidacloprid (K_d = 530 nM) and clothianidin (K_d = 1.79 μM) (Table 2). Entropy for thiacloprid was positive, while that for imidacloprid, clothianidin, and CH-IMI was negative (Table 2), consistent with distinct binding characteristics of thiacloprid from those of the other neonicotinoids.

Effects of the Gln55Arg mutation on AChBP–neonicotinoid interactions

We investigated the impact of the Gln55Arg mutation on AChBP–neonicotinoid interactions based on X-ray crystal structures of the ligand complexes. The Gln55Arg mutation had no major impact on the stacking with Tyr185 of the guanidine moiety of imidacloprid, clothianidin and CH-IMI. However, not only the NO_2 group of imidacloprid (Fig. 3B, C) and CH-IMI (Fig. 3K, L), but also of clothianidin (Fig. 3E, F) which had no contact with loop D in the wild-type protein, interacted electrostatically with the side chain of Arg55 in loop D. The most striking impact of the Gln55Arg mutation was observed in its interactions with thiacloprid. Although thiacloprid did not stack with Tyr185 in the wild-type protein (Fig. 3G)), it did stack with Tyr185, orienting the CN group toward Arg55 (Fig. 3H, I).

In response to the Gln55Arg mutation, neonicotinoid affinity was slightly enhanced or at least retained, whereas the affinity of (-)-nicotine (Table 2) was markedly reduced. Interestingly, the Gln55Arg mutation enhanced enthalpy and reduced entropy for thiacloprid, whereas the reverse was the case for clothianidin (Table 2).

Unique binding of DN-IMI to *Ls*-AChBP

DN-IMI is an imidacloprid metabolite lacking the negatively charged NO_2 group, which is an important structural feature of neonicotinoids. The removal of the NO_2 group results in a

Molecular Pharmacology Fast Forward. Published on September 29, 2014 as DOI: 10.1124/mol.114.094698
This article has not been copyedited and formatted. The final version may differ from this version.

positively charged guanidine group (Fig. 1A). DN-IMI interacted with the wild-type and Gln55Arg mutant of *Ls*-AChBPs in a completely different manner from the other neonicotinoids (Fig. 4). In the wild-type protein, DN-IMI stacked with Tyr185, yet directed its guanidine away from Gln55 (Fig. 4A), forming a hydrogen bond with Tyr89 in loop A and the main chain of Trp143 in loop B (Fig. 4A). The Gln55Arg mutation further induced a change of the stacking partner of DN-IMI from Tyr185 to Tyr192, retaining the hydrogen bond with Tyr89 and Trp143 (Fig. 4B, C) with increased entropy (Table 2).

Ligand interactions with a basic residue on the β1 strand

In addition to the anticipated interactions with loops A–F, we found for the first time that the NO_2 group in clothianidin (Fig. 5A) and the CN group in thiacloprid (Fig. 5B) interacted with Lys34, which corresponds to Ile44 in loop G on the β1 strand of the mouse serotonin 5-HT_3 receptor (Hassaine et al., 2014), in the Gln55Arg mutant. CH-IMI also interacted with Lys34 in the Gln55Arg mutant (Fig. 5C) as in the wild-type protein with the highest affinity (Table 2).

The effects of mutations of Ser55 and Gln79 to basic amino acids on the α7 nAChR responses to neonicotinoids, DN-IMI, (-)-nicotine and ACh

To clarify whether basic residues on the β1 strand, as well as the basic residues in loop D, play a key role in neonicotinoid actions on nAChRs, we employed the avian α7 nAChR because 1) it shows higher similarity than heteropentameric nAChRs to the *Ls*-AChBP in its amino acid sequence of the extracellular domain (for the avian α7, 26%; for the human α7, 24%) as well as in its ability to form a homopentamer (Brejc et al., 2001) and 2) higher neonicotinoid sensitivity than vertebrate heteropentameric nAChRs (Ihara et al., 2003) and thus has been used extensively in characterizing neonicotinoid actions (Ihara et al., 2003; Shimomura et al., 2002;

Molecular Pharmacology Fast Forward. Published on September 29, 2014 as DOI: 10.1124/mol.114.094698
This article has not been copyedited and formatted. The final version may differ from this version.

Shimomura et al., 2003). We mutated to basic residues Ser58 and Gln79 corresponding Lys34 and Gln55, respectively of the *Ls*-AChBP and investigated the effects of such mutations on agonist action of the ligands studied. All the ligands induced inward currents in oocytes expressing the wild-type and mutant α7 nAChRs (Fig. 6). Imidacloprid, clothianidin and thiacloprid were partial agonists, while CH-IMI, DN-IMI and (-)-nicotine were full or nearly full agonists (Fig. 7A). The Ser58Lys mutation selectively enhanced the efficacy in terms of I_{max} of neonicotinoids (Fig. 7B). Notably, imidacloprid, thiacloprid and CH-IMI showed greater I_{max} than ACh for the Ser58Lys mutant. In contrast, the Ser58Lys mutation reduced the affinity in pEC_{50} of ACh, (-)-nicotine and DN-IMI ($p < 0.05$, one way ANOVA, Dunnett's test). Similarly, the Gln79Arg mutation corresponding to the Gln55Arg mutation in the *Ls*-AChBP (Figure 7C) enhanced the efficacy of neonicotinoids, while reducing the affinity of ACh, (-)-nicotine and DN-IMI (Table 3).

When both Ser58 and Gln79 were mutated to basic residues, the pEC_{50} value of imidacloprid was significantly increased ($p < 0.05$, one way ANOVA, Dunnett's test) (Fig. 7D, Table 3). Also, the Ser58Lys;Gln79Arg double mutation resulted in enhanced I_{max} values of all the neonicotinoids tested compared to those obtained for wild-type α7, while significantly reducing the pEC_{50} values of ACh, (-)-nicotine and DN-IMI as well as the I_{max} values of (-)-nicotine and DN-IMI ($p < 0.05$, one way ANOVA, Dunnett's test). No significant effect of the mutations was observed on the decay time constant for the agonist-induced currents in *Xenopus* oocytes expressing α7 (data not shown).

Molecular Pharmacology Fast Forward. Published on September 29, 2014 as DOI: 10.1124/mol.114.094698
This article has not been copyedited and formatted. The final version may differ from this version.

Discussion

In this study, we employed the *Ls*-AChBP as a surrogate for the nAChR LBD, and co-crystallized with neonicotinoids both wild *Ls*-AChBP and its Gln55Arg mutant – the arginine residue at this loop D position being found in many insect nAChR LBDs (Fig. 1C). The resolution (2.09-2.68 Å) of these X-ray crystal structures are sufficient to model ligands and side chains/main chains involved in ligand binding. Such resolution also permits identification of water molecules including those involved in the aromatic ring nitrogen–loop E interactions (Supplementary Fig. 2) (Ihara et al., 2008), although such interactions with loop E would not directly contribute to the selective actions of neonicotinoids on insect nAChRs because similar interactions are also observed for (-)-nicotine (Celie et al., 2004) and epibatidine (Hansen et al., 2005).

We examined whether neonicotinoids generally stack with the tyrosine residue in loop C and interact electrostatically with the basic residue in loop D. Novel crystal structures of the wild-type and Gln55Arg mutant of the *Ls*-AChBP complexed with DN-IMI helped address whether the NO_2 group, so important in the actions of imidacloprid, is a key determinant of the interactions with loop D. Although thiacloprid did not stack with Tyr185 in loop C of the wild-type *Ls*-AChBP (Fig. 3G), it did stack with Tyr185 in the Gln55Arg mutant (Fig. 3H) as was the case for other neonicotinoids (Fig. 3B, E, K). The NO_2 group of clothianidin (Fig. 3D) and the CN group of thiacloprid (Fig. 3G) had no contact with Gln55 in the wild-type *Ls*-AChBP, apparently undermining the generalization that neonicotinoids interact with loop D. However, the Gln55Arg mutant induced stacking of both clothianidin and thiacloprid with Tyr185 in loop C. The Gln55Arg mutation also lead to electrostatic interactions of the clothianidin NO_2 group with the inserted basic residue, while breaking another hydrogen bond between the guanidine NH and the backbone carbonyl (Fig. 3E). In addition, this mutation

Molecular Pharmacology Fast Forward. Published on September 29, 2014 as DOI: 10.1124/mol.114.094698
This article has not been copyedited and formatted. The final version may differ from this version.

changed the orientation of the thiacloprid CN group from the main chain of loop C to Arg55 in loop D, demonstrating that the basic residue generally determines the binding mode of neonicotinoids at LBD. Nevertheless, the interactions with loop C cannot be ignored in the neonicotinoid actions because a glutamate residue in this loop of vertebrate nAChR α subunits (Fig. 1C) was shown to play a role in the low neonicotinoid sensitivity (Shimomura et al., 2004).

To investigate such Gln55Arg mutation-induced changes of the binding mode in another way, we measured the thermodynamic parameters by ITC for interactions of all the ligands studied with the wild-type and Gln55Arg mutant *Ls*-AChBPs. In the case of clothianidin, enthalpy was reduced, while entropy was increased in response to the Gln55Arg mutation, which may result from a break of the hydrogen bond with the main chain of Trp143 in loop B. On the other hand, the wild-type *Ls*-AChBP–thiacloprid interactions resulted in positive entropy, possibly reflecting dehydration of the functional group as a consequence of hydrogen bond formation with the main chain of loop C. The Gln55Arg mutation induced thiacloprid stacking with Tyr185, resulting in reduced mobility of the compound (Table 2), which may, at least in part, account for the reduced entropy.

In contrast with the effects on neonicotinoids, the Gln55Arg mutation reduced the affinity of (-)-nicotine (Table 2), suggesting a gate-keeper role for the basic residue that repels positively charged agonists. In the wild-type and the Gln55Arg mutant of *Ls*-AChBP, the positively charged guanidine of DN-IMI was oriented away from loop D (Fig. 4), supporting the critical role for neutral to negatively charged “nitro-” and “cyano-” groups of neonicotinoids.

Bass *et al*. (2011) found that the Arg81Thr mutation in loop D of the β1 subunit (Fig. 1C) conferred strong neonicotinoid resistance in the peach aphid *Myzus persicae* (Bass et al., 2011). The weakest impact of the Gln79Arg mutation on thiacloprid actions on α7 (Fig. 7C) is in

Molecular Pharmacology Fast Forward. Published on September 29, 2014 as DOI: 10.1124/mol.114.094698
This article has not been copyedited and formatted. The final version may differ from this version.

accord with the weakest electrostatic interactions between the CN group in thiacloprid and Arg55 in the Gln55Arg mutant *Ls*-AChBP (Fig. 3H). We therefore suggest that thiacloprid actions are less profoundly affected by this mutation than the actions of other neonicotinoids.

Unexpectedly, we found that Lys34 on the β1 strand in the complementary side contributes to the interactions of clothianidin, thiacloprid and CH-IMI with LBD (Fig. 5). We presumed that such a basic residue in loop G could also play a role in the selective actions of neonicotinoids and thus investigated agonist actions of neonicotinoids, DN-IMI, (-)-nicotine and ACh on the avian α7 nAChR mutagenized to yield basic residues at the equivalent position of Lys34. This resulted in significant impact on efficacy (Fig. 7, Table 3). No previous study has shown that any mutation of Ser58 and equivalent amino acids in loop G affects the selectivity and diversity of agonist actions on Cys-loop ligand-gated ion channels. CH-IMI contacted most strongly with Lys34 (Fig. 5C), accounting for the highest impact of the Ser58Lys mutation on its agonist actions on α7 (Fig. 7B) (Fig. 3). When combined with Arg79 (Fig. 7C), Lys58 exerted even more striking effect than the single mutation, not only on the affinity of imidacloprid, but also on the efficacy of all the ligands studied (Fig. 7D, Table 3). Presumably, similar results would also be observed with human α7, as it shares high similarity with the avian α7 (93.8% in the extracellular agonist binding regions; overall similarity, 89.9%). In future, it will be of interest to examine by a double mutant cycle analysis (Horovitz, 1996) whether there is any possible cooperativity of the two basic residues. Also, in future it will be necessary to examine whether the agonist profile of α7 concurs with that of robustly expressed insect nAChRs. Nevertheless, not only the interactions at the α–non-α subunit interface, but also those at the α–α subunit interface, may well underlie the neonicotinoid actions because the basic residue in loop G in the complementary side of the *Ls*-AChBP interacted with neonicotinoids and significantly enhanced the agonist actions of neonicotinoids on α7. In addition, we predict that neonicotinoid resistance

Molecular Pharmacology Fast Forward. Published on September 29, 2014 as DOI: 10.1124/mol.114.094698
This article has not been copyedited and formatted. The final version may differ from this version.

may occur in pest insect species by a mutation of the basic residue to serine in loop G (Fig. 1C) as in the case of the R81T mutation in loop D (Bass et al., 2011).

Honey bees (*Apis mellifera*) also possess the "canonical" two basic residues in both loops D and G of nAChRs other than those consisting of α5–α7 subunits (Fig. 1**C**), thereby showing some sensitivity to the commercial neonicotinoids. Thus it appears difficult to design pest-species-selective chemicals acting on the neonicotinoid-binding pocket in nAChRs. Nevertheless, the pocket in honey bee nAChRs has distinct size, electrostatic potentials and hydrogen-bond capability from that in pest insect species (Matsuda et al., 2009). Thus the structural data generated in this study may help in the design of compounds that are safer to mammals and beneficial insects.

In conclusion, we have identified structural determinants defining the interactions of neonicotinoids and DN-IMI with the wild-type and Gln55Arg mutant of *Ls*-AChBP. In addition to the basic residue in loop D, we newly found that Lys34 in loop G on the β1 strand also interacted with neonicotinoids in the *Ls*-AChBP and noted significant impact of the equivalent residue on the agonist actions of both neonicotinoids and other agonists on the homopentameric α7 nAChR. Thus we show that both loop D and loop G basic residues strengthen the nAChR–neonicotinoid interactions.

Molecular Pharmacology Fast Forward. Published on September 29, 2014 as DOI: 10.1124/mol.114.094698
This article has not been copyedited and formatted. The final version may differ from this version.

Acknowledgements

The authors acknowledge Dr. Takaaki Hikima and Dr. Go Ueno for help on data collection at BL44B2 and BL26B1/B2 beamlines at SPring-8, and Division of Instrumental Analysis, Okayama University, for support of X-ray diffraction data processing. Data collection at BL44XU beamline at SPring-8 was performed under the Cooperative Research Program of the Institute for Protein Research, Osaka University (Proposal No.: 2007A6904, 2007B6904). The authors thank Prof. Chojiro Kojima of Institute for Protein Research, Osaka University for assisting in the geometry analysis using Mogul. The authors also thank Prof. Seiki Kuramitsu of Department of Biological Sciences, Graduate School of Science, Osaka University and Ms Maiko Uozaki of DKSH Japan for measuring ITC of the compounds.

Authorship contribution

Participated in research design: Ihara, Yamashita, Okajima, Sattelle, Matsuda

Conducted experiments: Ihara, Yamashita, Okajima, Oda, Matsui, Asano, Matsuda

Performed data analysis: Ihara, Yamashita, Okajima, Oda, Matsui, Asano, Sattelle, Matsuda

Wrote the manuscript: Ihara, Yamashita, Okajima, Sattelle, Matsuda

References

Adachi S, Oguchi T, Tanida H, Park S-Y, Shimizu H, Miyatake H, Kamiya N, Shiro Y, Inoue Y, Ueki T and Iizuka T (2001) The RIKEN structural biology beamline II (BL44B2) at the SPring-8. *Nucl Instrum Methods Phys Res* **A467/A468**: 711-714.

Adams PD, Afonine PV, Bunkoczi G, Chen VB, Davis IW, Echols N, Headd JJ, Hung LW, Kapral GJ, Grosse-Kunstleve RW, McCoy AJ, Moriarty NW, Oeffner R, Read RJ, Richardson DC, Richardson JS, Terwilliger TC and Zwart PH (2010) PHENIX: a comprehensive Python-based system for macromolecular structure solution. *Acta Crystallogr D Biol Crystallogr* **66**: 213-221.

Bass C, Puinean AM, Andrews M, Cutler P, Daniels M, Elias J, Paul VL, Crossthwaite AJ, Denholm I, Field LM, Foster SP, Lind R, Williamson MS and Slater R (2011) Mutation of a nicotinic acetylcholine receptor beta subunit is associated with resistance to neonicotinoid insecticides in the aphid *Myzus persicae*. *BMC Neurosci* **12**: 51.

Brünger AT, Adams PD, Clore GM, DeLano WL, Gros P, Grosse-Kunstleve RW, Jiang JS, Kuszewski J, Nilges M, Pannu NS, Read RJ, Rice LM, Simonson T and Warren GL (1998) Crystallography & NMR system: A new software suite for macromolecular structure determination. *Acta Crystallogr D Biol Crystallogr* **54**: 905-921.

Brejc K, van Dijk WJ, Klaassen RV, Schuurmans M, van Der Oost J, Smit AB and Sixma TK (2001) Crystal structure of an ACh-binding protein reveals the ligand-binding domain of nicotinic receptors. *Nature* **411**: 269-276.

Bruno IJ, Cole JC, Kessler M, Luo J, Motherwell WD, Purkis LH, Smith BR, Taylor R, Cooper RI, Harris SE and Orpen AG (2004) Retrieval of crystallographically-derived molecular geometry information. *J Chem Inf Comput Sci* **44**: 2133-2144.

Casida JE and Durkin KA (2013) Neuroactive insecticides: targets, selectivity, resistance, and secondary effects. *Annu Rev Entomol* **58**: 99-117.

Celie PH, van Rossum-Fikkert SE, van Dijk WJ, Brejc K, Smit AB and Sixma TK (2004) Nicotine and carbamylcholine binding to nicotinic acetylcholine receptors as studied in AChBP crystal structures. *Neuron* **41**: 907-914.

Changeux JP (2012) The nicotinic acetylcholine receptor: the founding father of the pentameric ligand-gated ion channel superfamily. *J Biol Chem* **287**: 40207-40215.

Corringer PJ, Le Novere N and Changeux JP (2000) Nicotinic receptors at the amino acid level. *Annu Rev Pharmacol Toxicol* **40**: 431-458.

Couturier S, Bertrand D, Matter JM, Hernandez MC, Bertrand S, Millar N, Valera S, Barkas T and Ballivet M (1990) A neuronal nicotinic acetylcholine receptor subunit α7 is developmentally regulated and forms a homo-oligomeric channel blocked by α-BTX. *Neuron* **5**: 847-856.

Emsley P and Cowtan K (2004) Coot: model-building tools for molecular graphics. *Acta Crystallogr D Biol Crystallogr* **60**: 2126-2132.

Gill RJ, Ramos-Rodriguez O and Raine NE (2012) Combined pesticide exposure severely affects individual- and colony-level traits in bees. *Nature* **491**: 105-108.

Hallmann CA, Foppen RP, van Turnhout CA, de Kroon H and Jongejans E (2014) Declines in insectivorous birds are associated with high neonicotinoid concentrations. *Nature* **511**: 341-343.

Hansen SB, Sulzenbacher G, Huxford T, Marchot P, Taylor P and Bourne Y (2005) Structures of *Aplysia* AChBP complexes with nicotinic agonists and antagonists reveal distinctive binding interfaces and conformations. *EMBO J* **24**: 3635-3646.

Hassaine G, Deluz C, Grasso L, Wyss R, Tol MB, Hovius R, Graff A, Stahlberg H, Tomizaki T, Desmyter A, Moreau C, Li XD, Poitevin F, Vogel H and Nury H (2014) X-ray structure of the mouse serotonin 5-HT3 receptor. *Nature* **512**: 276-281.

Horovitz A (1996) Double-mutant cycles: a powerful tool for analyzing protein structure and function. *Fold Des* **1**: R121-126.

Hurst R, Rollema H and Bertrand D (2013) Nicotinic acetylcholine receptors: From basic science to therapeutics. *Pharmacol Ther* **137**: 22-54.

Ihara M, Brown LA, Ishida C, Okuda H, Sattelle DB and Matsuda K (2006) Actions of imidacloprid, clothianidin and related neonicotinoids on nicotinic acetylcholine receptors of American cockroach neurons and their relationships with insecticidal potency. *J Pestic Sci* **31**: 35-40.

Ihara M, Matsuda K, Otake M, Kuwamura M, Shimomura M, Komai K, Akamatsu M, Raymond V and Sattelle DB (2003) Diverse actions of neonicotinoids on chicken α7, α4β2 and *Drosophila*-chicken SADβ2 and ALSβ2 hybrid nicotinic acetylcholine receptors expressed in *Xenopus laevis* oocytes. *Neuropharmacology* **45**: 133-144.

Ihara M, Matsuda K, Shimomura M, Sattelle DB and Komai K (2004) Super agonist actions of clothianidin and related compounds on the SADβ2 nicotinic acetylcholine receptor expressed in *Xenopus laevis* oocytes. *Biosci Biotechnol Biochem* **68**: 761-763.

Ihara M, Okajima T, Yamashita A, Oda T, Hirata K, Nishiwaki H, Morimoto T, Akamatsu M, Ashikawa Y, Kuroda S, Mega R, Kuramitsu S, Sattelle DB and Matsuda K (2008) Crystal structures of *Lymnaea stagnalis* AChBP in complex with neonicotinoid insecticides imidacloprid and clothianidin. *Invert Neurosci* **8**: 71-81.

Latli B, C. T, Morimoto H, Williams PG and Casida JE (1996) [6-Chloro-3-pyridylmethyl-^{3}H]neonicotinoids as high-affinity radioligands for the nicotinic acetylcholine receptor: Preparationusing $NaB^{3}H_4$ and $LiB^{3}H_4$. *J Label Compd Radiopharm* **38**: 971-978.

Leslie AGW (1992) Recent changes to the MOSFLM package for processing film and image plate data. *Joint CCP4+ESF-EAMCB Newslett Prot Crystallogr* **26**.

Matsuda K, Buckingham SD, Kleier D, Rauh JJ, Grauso M and Sattelle DB (2001) Neonicotinoids: insecticides acting on insect nicotinic acetylcholine receptors. *Trends Pharmacol Sci* **22**: 573-580.

Matsuda K, Kanaoka S, Akamatsu M and Sattelle DB (2009) Diverse actions and target-site selectivity of neonicotinoids: structural insights. *Mol Pharmacol* **76**: 1-10.

Matsuda K, Shimomura M, Ihara M, Akamatsu M and Sattelle DB (2005) Neonicotinoids show selective and diverse actions on their nicotinic receptor targets: electrophysiology, molecular biology, and receptor modeling studies. *Biosci Biotechnol Biochem* **69**: 1442-1452.

Maus C, Curé G and Schmuck R (2003) Safety of imidacloprid seed dressings to honey bees: a comprehensive overview and compilation of the current state of knowledge. *Bull Insectol* **56**: 51-57.

McCoy AJ (2007) Solving structures of protein complexes by molecular replacement with Phaser. *Acta Crystallogr D Biol Crystallogr* **63**: 32-41.

Miller KG, Alfonso A, Nguyen M, Crowell JA, Johnson CD and Rand JB (1996) A genetic selection for Caenorhabditis elegans synaptic transmission mutants. *Proc Natl Acad Sci U S A* **93**: 12593-12598.

Nguyen M, Alfonso A, Johnson CD and Rand JB (1995) Caenorhabditis elegans mutants resistant to inhibitors of acetylcholinesterase. *Genetics* **140**: 527-535.

Nishio M (2006) The CH/π hydrogen bond: An important molecular force in controlling the crystal conformation of organic compounds and three-dimensional structure of biopolymers *Top Stereochem* **25**: 255-302.

Otwinowski Z and Minor W (1997) Processing of X-ray diffraction data collected in oscillation mode. *Methods Enzymol* **276**: 307-326.

PhillipsMcDougall (2013) *AgriReference*.

Rucktooa P, Smit AB and Sixma TK (2009) Insight in nAChR subtype selectivity from AChBP crystal structures. *Biochem Pharmacol* **78**: 777-787.

Salgado VL and Saar R (2004) Desensitizing and non-desensitizing subtypes of α-bungarotoxin-sensitive nicotinic acetylcholine receptors in cockroach neurons. *J Insect Physiol* **50**: 867-879.

Shimomura M, Okuda H, Matsuda K, Komai K, Akamatsu M and Sattelle DB (2002) Effects of mutations of a glutamine residue in loop D of the α7 nicotinic acetylcholine receptor on agonist profiles for neonicotinoid insecticides and related ligands. *Br J Pharmacol* **137**: 162-169.

Shimomura M, Yokota M, Ihara M, Akamatsu M, Sattelle DB and Matsuda K (2006) Role in the selectivity of neonicotinoids of insect-specific basic residues in loop D of the nicotinic acetylcholine receptor agonist binding site. *Mol Pharmacol* **70**: 1255-1263.

Shimomura M, Yokota M, Matsuda K, Sattelle DB and Komai K (2004) Roles of loop C and the loop B-C interval of the nicotinic receptor α subunit in its selective interactions with imidacloprid in insects. *Neurosci Lett* **363**: 195-198.

Shimomura M, Yokota M, Okumura M, Matsuda K, Akamatsu M, Sattelle DB and Komai K (2003) Combinatorial mutations in loops D and F strongly influence responses of the α7 nicotinic acetylcholine receptor to imidacloprid. *Brain Res* **991**: 71-77.

Talley TT, Harel M, Hibbs RE, Radic Z, Tomizawa M, Casida JE and Taylor P (2008) Atomic interactions of neonicotinoid agonists with AChBP: molecular recognition of the distinctive electronegative pharmacophore. *Proc Natl Acad Sci U S A* **105**: 7606-7611.

Tomizawa M and Casida JE (2003) Selective toxicity of neonicotinoids attributable to specificity of insect and mammalian nicotinic receptors. *Annu Rev Entomol* **48**: 339-364.

Tomizawa M and Casida JE (2005) Neonicotinoid insecticide toxicology: mechanisms of selective action. *Annu Rev Pharmacol Toxicol* **45**: 247-268.

Toshima K, Kanaoka S, Yamada A, Tarumoto K, Akamatsu M, Sattelle DB and Matsuda K (2009) Combined roles of loops C and D in the interactions of a neonicotinoid insecticide imidacloprid with the α4β2 nicotinic acetylcholine receptor. *Neuropharmacology* **56**: 264-272.

Ueno G, Kanda H, Hirose R, Ida K, Kumasaka T and Yamamoto M (2006) RIKEN structural genomics beamlines at the SPring-8; high throughput protein crystallography with automated beamline operation. *J Struct Funct Genomics* **7**: 15-22.

Unwin N and Fujiyoshi Y (2012) Gating movement of acetylcholine receptor caught by plunge-freezing. *J Mol Biol* **422**: 617-634.

Vagin A and Teplyakov A (1997) MOLREP: an automated program for molecular replacement. *J Appl Crystallogr* **30**: 1022-1025.

Winn MD, Ballard CC, Cowtan KD, Dodson EJ, Emsley P, Evans PR, Keegan RM, Krissinel EB, Leslie AG, McCoy A, McNicholas SJ, Murshudov GN, Pannu NS, Potterton EA, Powell HR, Read RJ, Vagin A and Wilson KS (2011) Overview of the CCP4 suite and current developments. *Acta Crystallogr D Biol Crystallogr* **67**: 235-242.

Yoshimura M, Yamashita E, Suzuki M, Yamamoto M, Yoshikawa S, Tsukihara T and Nakagawa A (2007) Synchrotoron radiation instrumentation, in *Synchrotron Radiation Instrumentation: Ninth International Conference* (Rah Y-YCaS ed) pp 1916-1919.

Molecular Pharmacology Fast Forward. Published on September 29, 2014 as DOI: 10.1124/mol.114.094698
This article has not been copyedited and formatted. The final version may differ from this version.

FOOTNOTES

This study was supported by the Ministry of Agriculture, Forestry, and Fisheries of Japan Genomics-based Technology for Agricultural Improvement [Grant PRM-3002]; and the Strategic Project to Support the Formation of Research Bases at Private Universities: Matching Fund Subsidy from the Ministry of Education, Culture, Sports, Science and Technology of Japan [Grant S1101035].

Makoto Ihara, Toshihide Okajima and Atsuko Yamashita contributed equally to this study.

Molecular Pharmacology Fast Forward. Published on September 29, 2014 as DOI: 10.1124/mol.114.094698
This article has not been copyedited and formatted. The final version may differ from this version.

Figure legends

Figure 1. Chemical structures of acetylcholine, (-)-nicotine and neonicotinoids; sequence alignments of *Lymnaea stagnalis* (*Ls*)-AChBP and LBD of α7; alignments of loop D and β1 strand of AChBPs and nAChRs; whole view of Gln55Arg mutant of *Ls*-AChBP in complex with imidacloprid. (A) Chemical structures of acetylcholine (ACh), (-)-nicotine, neonicotinoids [Imidacloprid (IMI), clothianidin (CTD), thiacloprid (THI) and a nitromethylene imidacloprid analogue (CH-IMI)] and desnitro-imidacloprid (DN-IMI). (B) Pairwise alignment of *Lymnaea stagnalis* (*Ls*)-AChBP and chicken α7 nAChR. The secondary structures are illustrated above the primary structures. Positions of the binding site "loops A–F" are shown by horizontal bold lines. Residues Gln55 (corresponding to Gln79 of α7 nAChR) and Lys34 (Ser58 of α7) are colored red and arrowed. (C) Multiple sequence alignment of loop D and loop G of insect and vertebrate nAChR subunits alongside *Ls*-AChBP. Numbers indicate the position counted from the N-terminal Met1 of each nAChR subunit sequence, whereas those of *Ls*-AChBP indicate the position from the mature N-terminal. (D) The whole structure of Gln55Arg mutant of *Ls*-AChBP in complex with CH-IMI. CH-IMI, Lys34 (in sky blue) and Arg55 (in magenta) are drawn by space-fill models. Carbons, nitrogen, oxygen and chlorine atoms of CH-IMI are colored bright grey, blue, red and green, respectively.

Figure 2. F_o-F_c omit maps for bound neonicotinoids in the Gln55Arg mutant of *Ls*-AChBP. The simulated annealing F_o-F_c omit maps (blue) for imidacloprid (A), clothianidin (B), thiacloprid (C), CH-IMI (D) and DN-IMI (E) bound to the Gln55Arg mutant of *Ls*-AChBP are drawn with the final model. The omit maps for imidacloprid, thiacloprid, CH-IMI and DN-IMI are contoured at 3 σ, while that for clothianidin is contoured at 3.5 σ. In (B), an anomalous map of bromine atom contoured at 5.0 σ from an isomorphous crystal of the Gln55Arg mutant of the *Ls*-AChBP complexed with Br-clothianidin was overlaid. In (C), the anomalous maps

(orange) of sulfur and chlorine atoms contoured at 3.0 σ are overlaid. In each ligand, carbon, chlorine, nitrogen, oxygen and sulfur atoms are colored bright grey, green, blue, red and yellow, respectively.

Figure 3. Ligand binding domain of wild-type and Gln55Arg mutant of *Ls*-AChBP in complex with neonicotinoids. (A) Wild-type *Ls*-AChBP–imidacloprid complex, (B) Gln55Arg *Ls*-AChBP mutant–imidacloprid complex, (D) wild-type *Ls*-AChBP–clothianidin complex, (E) Gln55Arg *Ls*-AChBP mutant–clothianidin complex, (G) wild-type *Ls*-AChBP–thiacloprid complex, (H) Gln55Arg *Ls*-AChBP mutant–thiacloprid complex, (J) wild-type *Ls*-AChBP–nitromethylene imidacloprid analogue (CH-IMI) complex and (K) Gln55Arg *Ls*-AChBP mutant–CH-IMI complex. Abbreviations: Imidacloprid, IMI; clothianidin, CTD; thiacloprid, THI; nitromethylene imidacloprid analogue, CH-IMI. Carbon, chlorine, nitrogen, oxygen and sulfur atoms of the ligands are colored bright grey, green, blue, red and yellow, respectively. The binding site of imidacloprid (A, B) is represented by the subunit AB interface. The clothianidin-binding site of the wild-type (D) and Gln55Arg mutant (E) are represented by the subunit EA and CD interfaces, respectively. The binding sites of thiacloprid (G, H) and CH-IMI (J, K) are represented by the subunit EA and CD interfaces, respectively. The carbon atoms of the principal chains are colored bright pink, whereas those of the complementary chain are colored cyan. Panels A and D were generated using PDB data (PDB entry codes: 2ZJU, 2ZJV, respectively) reported in previous study (Ihara et al., 2008). The binding sites of the wild-type (light green) are superimposed on those of the Gln55Arg mutant (violet) in imidacloprid (C), clothianidin (F), thiacloprid (I) and CH-IMI (L) complexes. The coordinate data of the principal chain is used for superposition of the binding sites of the wild-type and Gln55Arg mutant *Ls*-AChBP. Bright blue and orange broken lines depict hydrogen bonds and electrostatic interactions, respectively.

Molecular Pharmacology Fast Forward. Published on September 29, 2014 as DOI: 10.1124/mol.114.094698
This article has not been copyedited and formatted. The final version may differ from this version.

Figure 4. Crystal structures of wild-type and Gln55Arg mutant *Ls*-AChBP in complex with desnitro-imidacloprid (DN-IMI). The binding sites of wild-type (A) and the Gln55Arg mutant (B) *Ls*-AChBPs are represented by the subunit AB interface. The carbon atoms of the principal chain are colored bright pink, whereas those of the complementary chain are colored cyan. The binding sites of the wild-type (light green) are superimposed on those of the Gln55Arg mutant (magenta) (C). In DN-IMI, chlorine, nitrogen and oxygen atoms are colored green, blue and red, respectively, whereas the carbon atoms are colored bright grey. Bright blue broken lines depict hydrogen bonds. For Gln55Arg mutant, three among the five ligand binding sites exhibit the same ligand binding configuration shown in the figure.

Figure 5. Expanded view of neonicotinoid-binding sites of the Gln55Arg mutant of *Ls*-AChBP. The binding sites of clothianidin (A), thiacloprid (B), and the nitromethylene imidacloprid analogue (CH-IMI) (C) on the Gln55Arg mutant of *Ls*-AChBP. The subunit BC interface is shown and interactions of the neonicotinoids with loop C, Arg55 in loop D on the β2 strand and Lys34 in loop G on the β1 strand are highlighted. Three (for clothianidin), four (for thiacloprid), and three (for CH-IMI) among the five ligand binding sites exhibited the distinct salt bridge formation with the distances less than 4 Å, as shown in the figures. The carbon atoms of the principal chains are colored bright pink, whereas those of the complementary chain are colored cyan. In the bound neonicotinoids, carbon, chlorine, nitrogen, oxygen and sulfur atoms are colored bright grey, green, blue, red and yellow, respectively. Orange broken lines depict hydrogen bonds/electrostatic interactions. See Supplementary Fig. 4 for electron-density map and the distribution of the B-factor for the Gln55Arg mutant–clothianidin complex.

Molecular Pharmacology Fast Forward. Published on September 29, 2014 as DOI: 10.1124/mol.114.094698
This article has not been copyedited and formatted. The final version may differ from this version.

Figure 6. Current responses to ACh, imidacloprid, clothianidin, thiacloprid, CH-IMI, DN-IMI and (-)-nicotine of wild-type and mutant (Ser58Lys, Gln79Arg and Ser58Lys;Gln79Arg) α7 nAChRs expressed in *Xenopus laevis* oocytes. Typical responses to the applied ligands are indicated.

Figure 7. Concentration-response curves showing agonist actions of acetylcholine, neonicotinoids [imidacloprid, clothianidin, thiacloprid, nitromethylene imidacloprid analogue (CH-IMI)], desnitro-imidacloprid (DN-IMI) and (-)-nicotine on wild-type and mutant α7 nicotinic acetylcholine receptors (α7 nAChRs) expressed in *Xenopus laevis* oocytes. Examples of the responses of α7 are shown in Fig. 7). Normalized peak current amplitude of the responses of α7 nAChRs were plotted against concentrations of the ligands tested. Each plot represents mean ± stand error of the mean of repeated experiments (n = 4–6). (A) Wild-type, (B) Ser58Lys mutant, (C) Gln79Arg mutant, (D) Ser58Lys;Gln79Arg double mutant. Ser58 and Gln79 correspond to Lys34 and Gln55 of *Ls*-AChBP, respectively. Note that the Ser58Lys (B) and Ser58Lys;Gln79Arg mutants (D) of α7 nAChR correspond to the wild-type and Gln55Arg mutant of *Ls*-AChBP. See Table 3 for affinity (pEC_{50}) and efficacy (I_{max}) of ligands obtained by fitting the concentration-response curves.

Table 1. X-ray diffraction data collection and refinement statistics for *L*-AChBP-neonicotinoid[a] complexes

	Gln55Arg mutant Imidacloprid	Gln55Arg mutant Clothianidin	Wild-type Thiacloprid	Gln55Arg mutant Thiacloprid	Wild-type CH-IMI	Gln55Arg mutant CH-IMI	Wild-type DN-IMI	Gln55Arg mutant DN-IMI	Gln55Arg mutant Br-Clothianidin (Br ano)[h]	Wild-type Thiacloprid (S ano)[h]	Gln55Arg mutant Thiacloprid (S ano)[h]
Data collection											
Beamline[b]	BL44XU	BL44XU	BL44B2	BL44XU	BL44B2	BL44XU	BL44B2	BL26B2	BL44B2	BL44B2	BL44B2
Wavelength (Å)	0.9	0.9	0.919	0.9	0.919	0.9	0.9	0.9	0.919	1.75	1.75
Space group	$P6_5$	$P6_5$	$P6_5$	$P6_5$	$P6_5$	$P6_5$	$P2_12_12_1$	$P2_12_12_1$	$P6_5$	$P6_5$	$P6_5$
Cell dimensions *a*, *b*, *c* (Å)	74.6, 74.6, 350.7	74.1, 74.1, 351.6	74.5, 74.5, 351.0	74.5, 74.5, 350.8	75.0, 75.0, 351.0	74.8, 74.8, 351.4	77.0, 118.4, 243.6	73.1, 120.7, 133.3	74.8 74.8 351.8	74.6, 74.6, 351.2	74.6, 74.6, 350.9
Resolution (Å)	18.1-2.52	39.6-2.67	47.5-2.24	39.6-2.68	47.6-2.30	18.0-2.48	50.0-2.09	50.0-2.25	50-3.2	50.0-2.90	50.0-3.0
R_{sym} (%)[c, d]	8.7 (40.0)	9.4 (40.2)	9.1(43.8)	8.4 (40.3)	7.7 (41.4)	9.9 (37.5)	7.4 (46.3)	7.6 (44.9)	13.8 (36.2)	10.3 (30.8)	8.9(34.0)
I/σ^{χ}	8.4 (1.9)	6.9 (1.8)	37.2 (5.20)	7.8 (1.8)	24.9 (2.42)	6.4 (2.0)	24.7 (2.30)	38.5 (4.44)	19.4 (8.4)	64.7 (16.5)	47.8(11.5)
Completeness	99.7 (100)	99.6 (99.9)	99.9 (100)	98.9 (99.9)	99.0 (91.1)	99.5 (99.5)	99.2 (93.7)	99.8 (99.7)	100 (100)	99.8 (99.6)	95.3(97.4)
Redundancy[b]	5.1 (5.1)	3.4 (3.4)	11.2 (10.3)	2.6 (2.6)	10.9 (7.9)	5.2 (5.2)	7.1 (6.4)	7.3 (7.0)	14.6 (14.8)	22.1 (22.0)	22.8(23.2)
Refinement											
Resolution (Å)	18.1-2.54	39.6-2.68	47.5-2.24	39.6-2.69	47.6-2.30	18.0-2.48	47.8-2.09	20.8-2.25			
No. reflections	35965	30443	52420	30084	48471	37741	131114	58862			
R/R_{free} (%)[e]	19.7/27.1	19.3/26.0	22.2/26.6	20.0/27.4	21.0/26.5	20.3/26.2	21.3/26.2	21.5/26.2			
Bond length (Å)/angles (deg)[f]	0.008/1.3 (0.004/0.29)	0.007/1.3 (0.001/0.16)	0.007/1.3 (0.004/0.25)	0.008/1.3 (0.004/0.31)	0.006/1.3 (0.003/0.15)	0.008/1.6 (0.003/0.14)	0.006/1.3 (0.003/0.16)	0.007/1.4 (0.004/0.25)			
Protein (ligands)											
B factor	38.9	48.0	38.2	46.9	40.7	37.3	38.5	43.8			
Protein (ligands)	(39.0)	(50.1)	(41.1)	(4837)	(32.0)	(28.6)	(31.1)	(29.8)			
PDB code[g]	3WTH	3WTI	3WTJ	3WTK	3WTL	3WTM	3WTN	3WTO			

[a]See text for abbreviations of the neonicotinoid names.

[b]All data sets were collected at SPring-8.

[c]Values in parentheses refer to data in the highest resolution shells.

[d]$R_{sym} = \Sigma|I-\langle I\rangle|/\Sigma I$, where I is the observed intensity and $\langle I\rangle$ is the average intensity from multiple observations of the symmetry related reflections.

[e]$R = \Sigma||F_o| - |F_c|| / \Sigma|F_o|$. R_{free} is an R factor of the CNS refinement evaluated for 5% of reflections that were excluded from the refinement.

[f]R.m.s. deviations from ideal values were calculated using either CNS, CCP4, or PHENIX for the protein parts, and Mogul for the ligand parts.

[g]The atomic coordinates and structure factors have been deposited in the Protein Data Bank.

[h]Data sets for detection of anomalous peaks at sulfur, bromine and chlorine atoms.

Table 2. K_d, ΔH and ΔS as determined by isothermal titration calorimetry

Compounds	K_d (μM)		ΔH (kcal/mol)		ΔS (cal/mol/K)	
	Wild-type	Gln55Arg mutant	Wild type	Gln55Arg mutant	Wild-type	Gln55Arg mutant
Imidacloprid	0.530 ± 0.023[a]	0.514 ± 0.053	-10.33 ± 0.11	-10.50 ± 0.21	-5.93 ± 0.39	-6.38 ± 0.89
Clothianidin	1.79 ± 0.05	1.27 ± 0.15	-9.85 ± 0.09	-6.28 ± 0.41	-6.74 ± 0.33	+5.97 ± 1.61
Thiacloprid	0.297 ± 0.012	0.294 ± 0.015	-6.87 ± 0.09	-11.49 ± 0.06	+6.84 ± 0.37	-8.62 ± 0.24
CH-IMI	0.092 ± 0.004	0.100 ± 0.003	-12.93 ± 0.92	-13.28 ± 0.46	-7.45 ± 0.61	-15.00 ± 1.47
DN-IMI	0.091 ± 0.004	0.119 ± 0.003	-12.84 ± 0.22	-10.74 ± 0.30	-10.78 ± 0.69	-4.32 ± 1.05
(-)-Nicotine	0.114 ± 0.017	0.609 ± 0.012	-15.07 ± 0.07	-14.45 ± 0.19	-18.97 ± 0.26	-20.03 ± 0.64

[a]Data are represented as means ± standard error of means from three replicates.

Molecular Pharmacology Fast Forward. Published on September 29, 2014 as DOI: 10.1124/mol.114.094698
This article has not been copyedited and formatted. The final version may differ from this version.

Table 3. pEC_{50} and I_{max} values of neonicotinoids and DN-IMI for the wild-type and mutant chicken α7 nicotinic acetylcholine receptors expressed in *Xenopus laevis* oocytes

Ligands	Wild-type		Ser58Lys mutant	
	pEC_{50}[a]	I_{max}[a]	pEC_{50}	I_{max}
Acetylcholine	3.82 ± 0.07	1.22 ± 0.05	1.82 ± 0.17	2.41 ± 0.39
Imidacloprid	3.67 ± 0.08	0.51 ± 0.03	ND[b]	23.1 ± 1.5[c]
Clothianidin	3.42 ± 0.18	0.16 ± 0.03	3.44 ± 1.37	1.72 ± 0.16
Thiacloprid	4.38 ± 0.17	0.49 ± 0.05	4.11 ± 0.10	3.15 ± 0.20
CH-IMI	4.42 ± 0.16	1.43 ± 0.12	4.67 ± 0.10	24.7 ± 1.2
DN-IMI	5.46 ± 0.09	1.00 ± 0.04	4.02 ± 0.03	2.45 ± 0.07
(-)-Nicotine	4.93 ± 0.03	0.88 ± 0.02	3.69 ± 0.05	0.15 ± 0.01
Ligands	Gln79Arg mutant		Ser58Lys;Gln79Arg mutant	
	pEC_{50}	I_{max}	pEC_{50}	I_{max}
Acetylcholine	2.63 ± 0.05	1.11 ± 0.03	2.14 ± 0.04	1.62 ± 0.06
Imidacloprid	4.02 ± 0.10	1.48 ± 0.11	4.16 ± 0.16	4.48 ± 0.45
Clothianidin	3.55 ± 0.05	1.04 ± 0.05	3.70 ± 0.09	2.84 ± 0.19
Thiacloprid	3.89 ± 0.06	0.30 ± 0.01	4.36 ± 0.17	5.53 ± 0.52
CH-IMI	4.89 ± 0.16	3.13 ± 0.21	5.02 ± 0.28	8.72 ± 0.95
DN-IMI	4.39 ± 0.05	0.67 ± 0.02	3.99 ± 0.02	0.69 ± 0.02
(-)-Nicotine	3.71 ± 0.07	0.35 ± 0.02	3.58 ± 0.14	0.10 ± 0.01

[a]All the data were newly measured. pEC_{50} is -log EC_{50} (Half maximal effective concentration (M)), whereas I_{max} is normalized maximal response. Data are represented as means ± standard error of 4–6 replicates.

[b]Could not be determined because the concentration-response curve did not reach a maximum.

[c]I_{max} was determined at 3 mM.

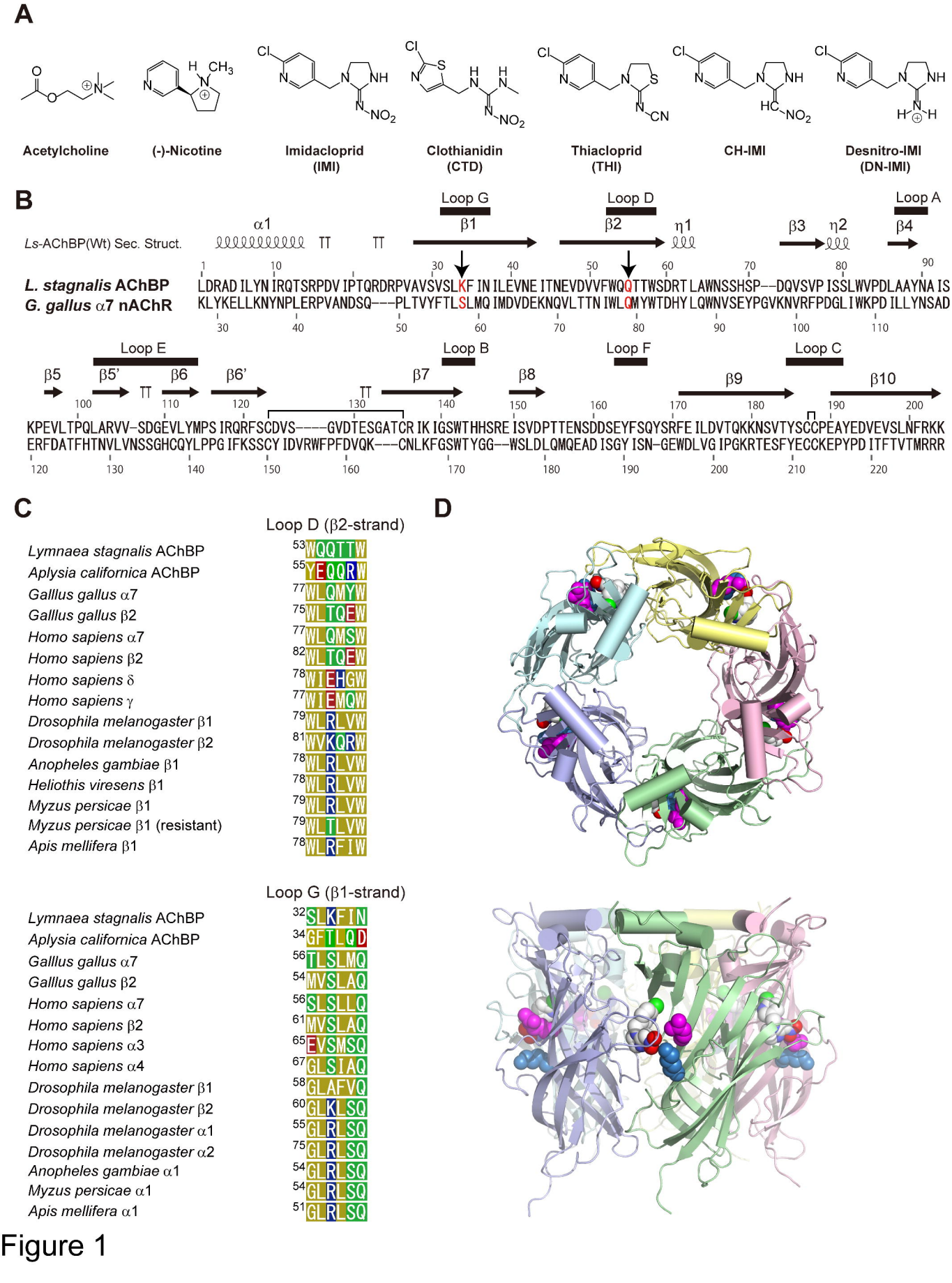
A
Acetylcholine
(-)-Nicotine
Imidacloprid (IMI)
Clothianidin (CTD)
Thiacloprid (THI)
CH-IMI
Desnitro-IMI (DN-IMI)
B
Ls-AChBP(Wt) Sec. Struct.
Loop G
Loop D
Loop A
Loop E
Loop B
Loop F
Loop C
L. stagnalis AChBP
G. gallus α7 nAChR
C
Loop D (β2-strand)
Lymnaea stagnalis AChBP
Aplysia californica AChBP
Galllus gallus α7
Galllus gallus β2
Homo sapiens α7
Homo sapiens β2
Homo sapiens δ
Homo sapiens γ
Drosophila melanogaster β1
Drosophila melanogaster β2
Anopheles gambiae β1
Heliothis viresens β1
Myzus persicae β1
Myzus persicae β1 (resistant)
Apis mellifera β1
Loop G (β1-strand)
Lymnaea stagnalis AChBP
Aplysia californica AChBP
Galllus gallus α7
Galllus gallus β2
Homo sapiens α7
Homo sapiens β2
Homo sapiens α3
Homo sapiens α4
Drosophila melanogaster β1
Drosophila melanogaster β2
Drosophila melanogaster α1
Drosophila melanogaster α2
Anopheles gambiae α1
Myzus persicae α1
Apis mellifera α1
D

Figure 1

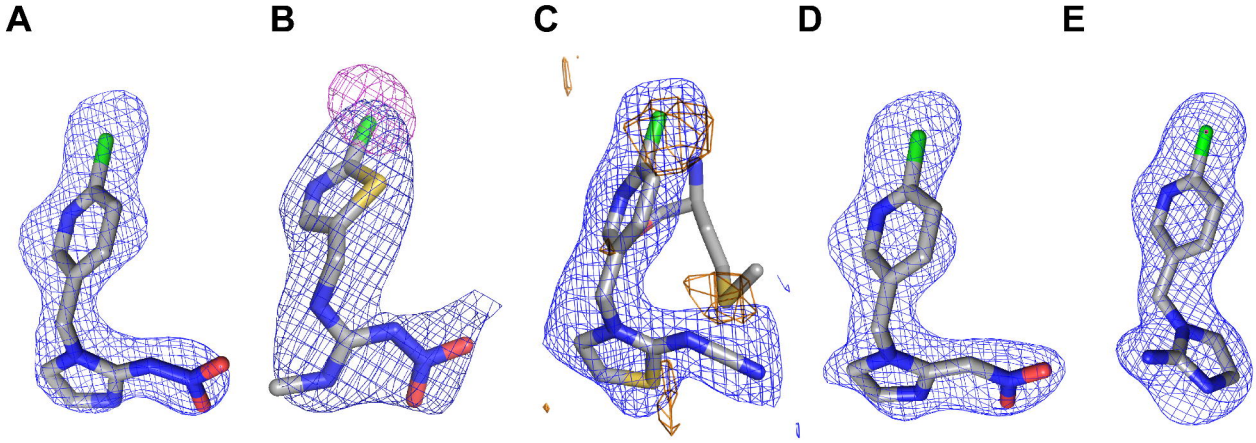

Figure 2

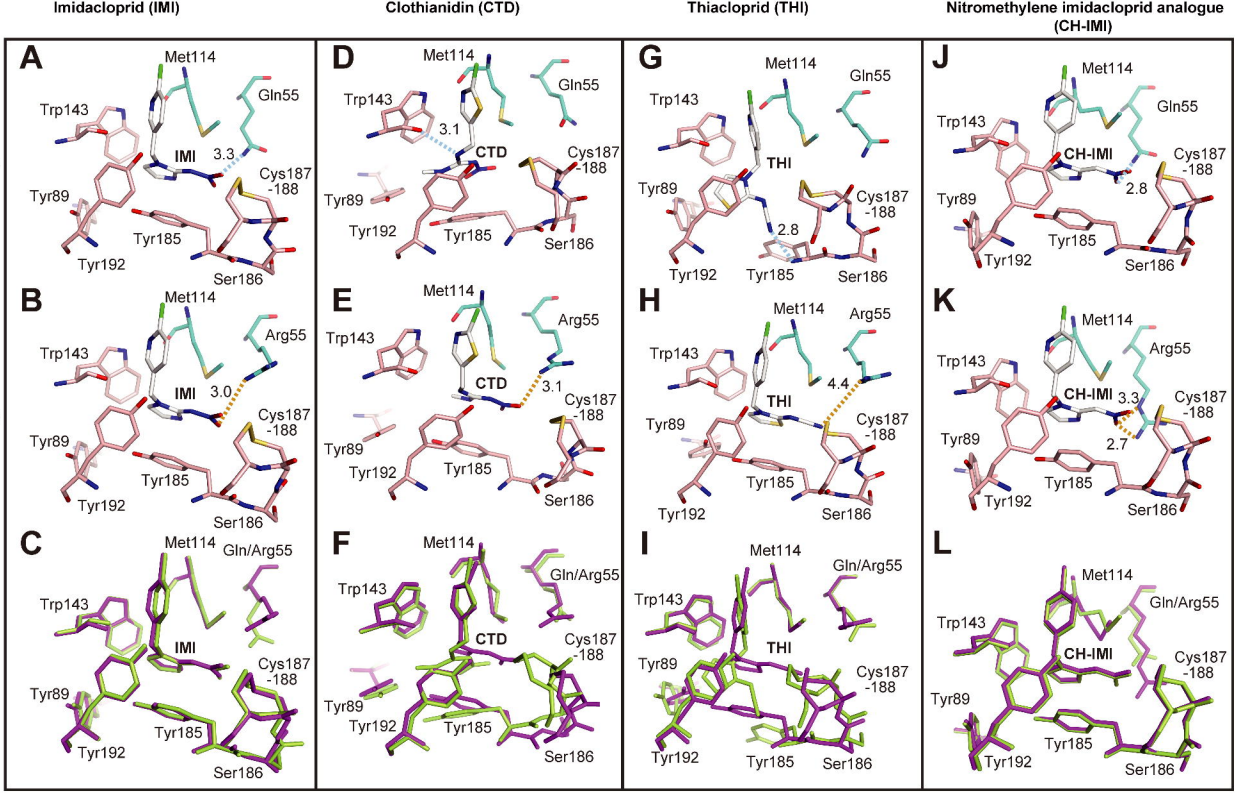
Imidacloprid (IMI)
Clothianidin (CTD)
Thiacloprid (THI)
Nitromethylene imidacloprid analogue (CH-IMI)
Wild-type
Gln55Arg mutant
Superposition
A
B
C
D
E
F
G
H
I
J
K
L
Met114
Gln55
Arg55
Gln/Arg55
Trp143
Tyr89
Tyr185
Tyr192
Ser186
Cys187 -188
IMI
CTD
THI
CH-IMI
3.3
3.0
3.1
2.8
4.4
2.7

Figure 3

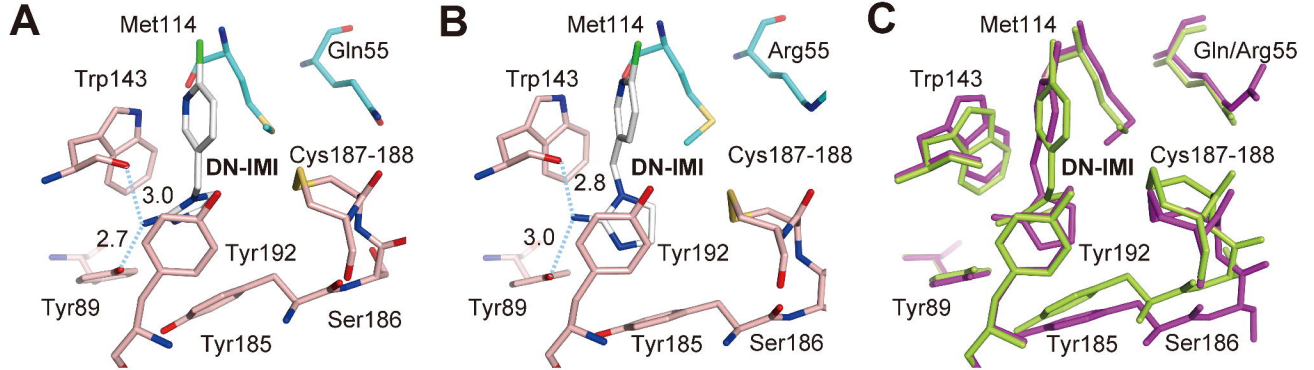
A
Met114
Gln55
Trp143
DN-IMI
Cys187-188
3.0
2.7
Tyr192
Tyr89
Ser186
Tyr185
B
Met114
Arg55
Trp143
DN-IMI
Cys187-188
2.8
3.0
Tyr192
Tyr89
Tyr185
Ser186
C
Met114
Gln/Arg55
Trp143
DN-IMI
Cys187-188
Tyr192
Tyr89
Tyr185
Ser186

Figure 4

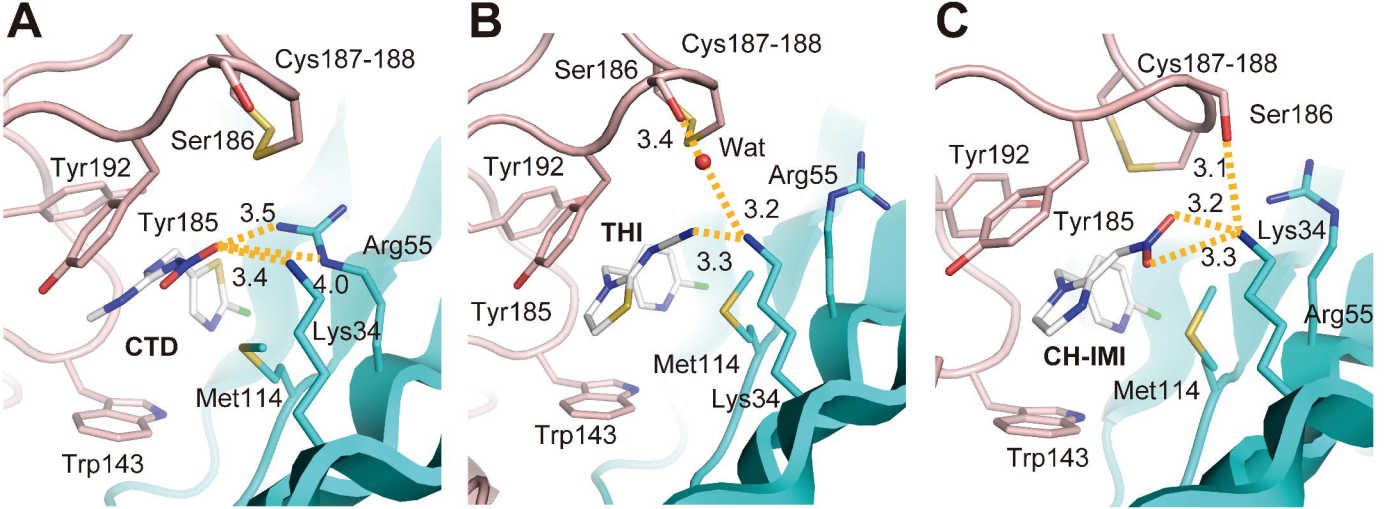
A
Cys187-188
Ser186
Tyr192
Tyr185
3.5
Arg55
3.4
4.0
CTD
Lys34
Met114
Trp143
B
Cys187-188
Ser186
3.4
Wat
Tyr192
Arg55
3.2
THI
3.3
Tyr185
Met114
Lys34
Trp143
C
Cys187-188
Ser186
Tyr192
3.1
3.2
Tyr185
Lys34
3.3
Arg55
CH-IMI
Met114
Trp143

Figure 5

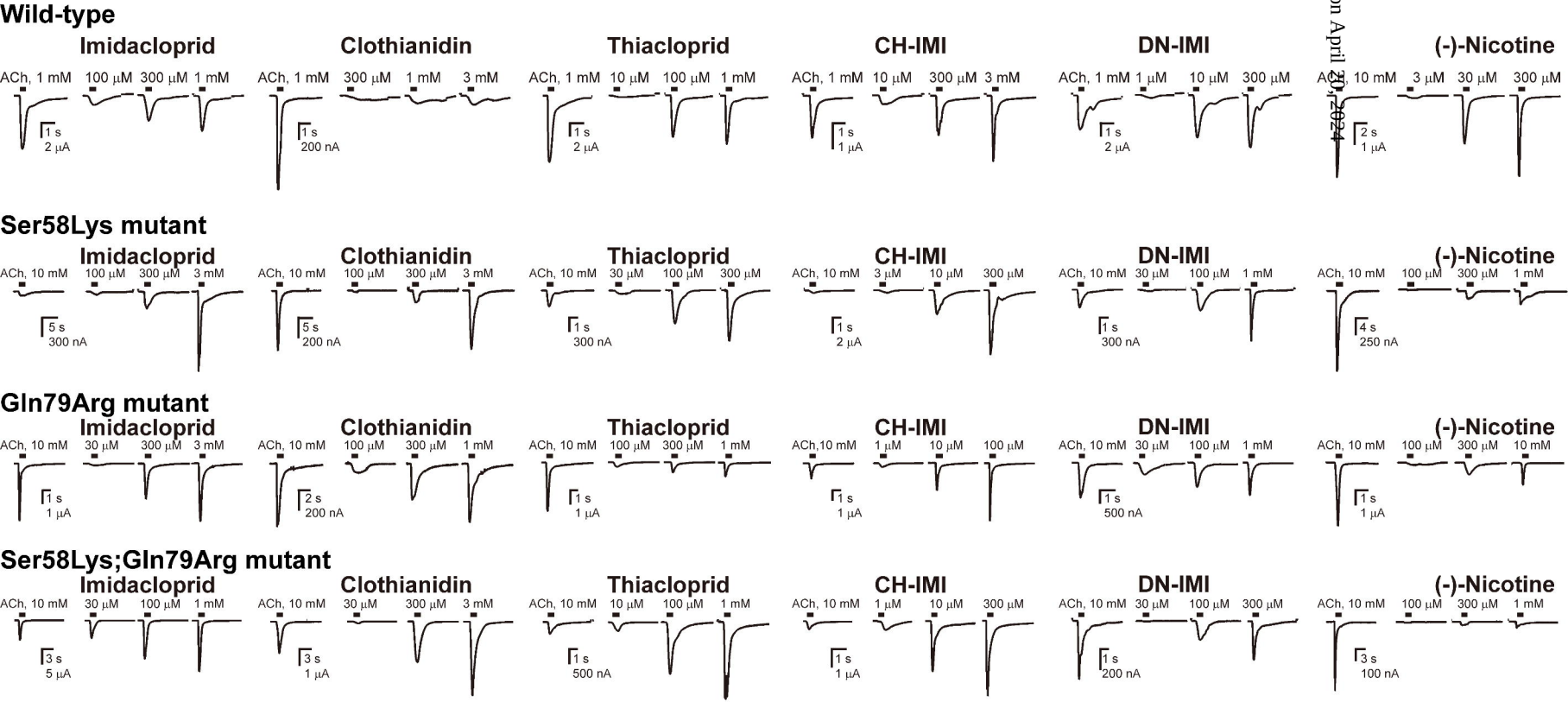

Figure 6

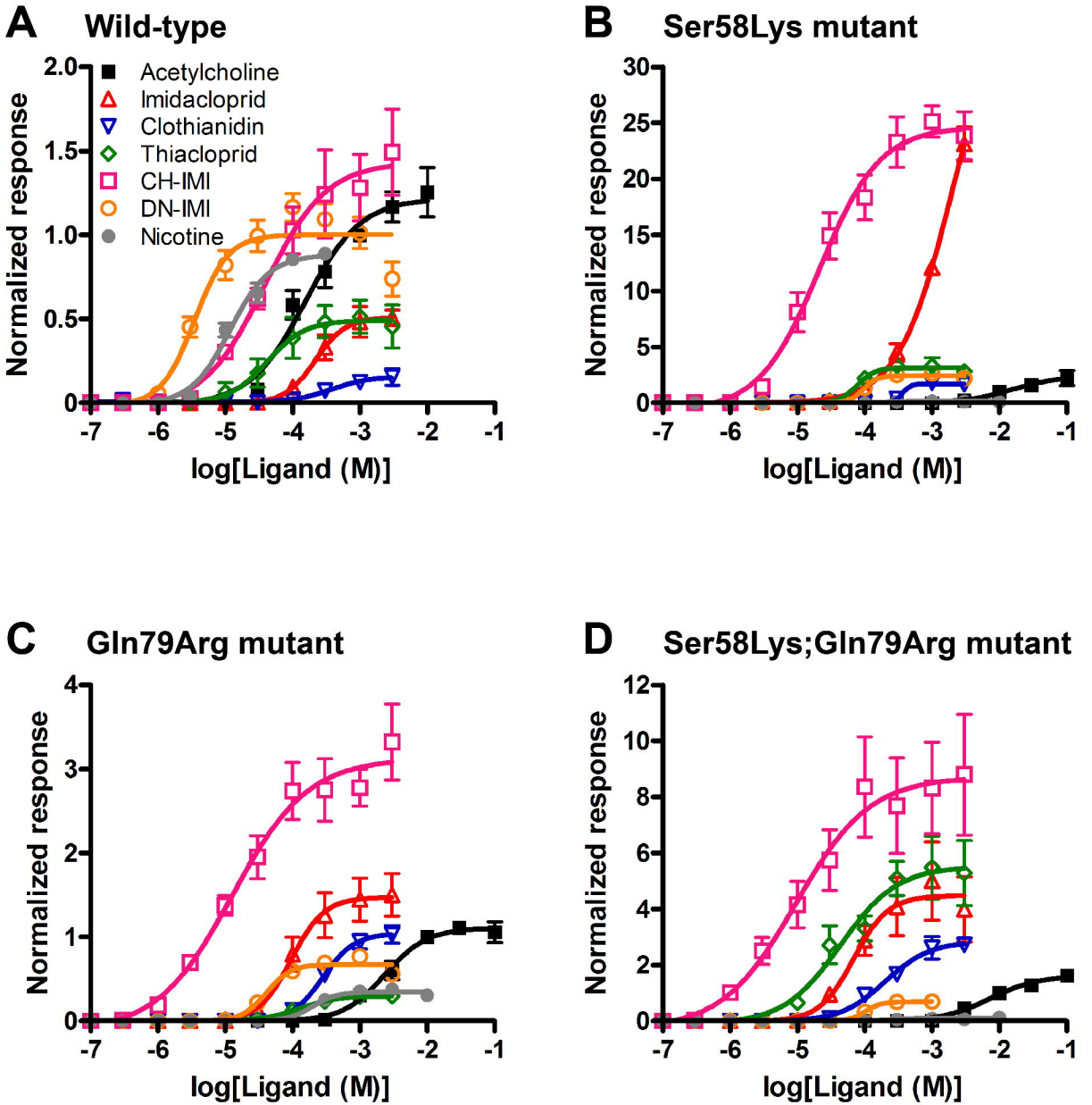
A
Wild-type
Acetylcholine
Imidacloprid
Clothianidin
Thiacloprid
CH-IMI
DN-IMI
Nicotine
Normalized response
log[Ligand (M)]
B
Ser58Lys mutant
Normalized response
log[Ligand (M)]
C
Gln79Arg mutant
Normalized response
log[Ligand (M)]
D
Ser58Lys;Gln79Arg mutant
Normalized response
log[Ligand (M)]

Figure 7